A general mechanism of polycrystalline growth

LÁSZLÓ GRÁNÁSY[1]*, TAMÁS PUSZTAI[1], TAMÁS BÖRZSÖNYI[1], JAMES A. WARREN[2] AND JACK F. DOUGLAS[3]

[1]Research Institute for Solid State Physics and Optics, PO Box 49, H-1525 Budapest, Hungary
[2]Metallurgy and [3]Polymers Divisions, National Institute of Standards and Technology, Gaithersburg, Maryland 20899, USA
*e-mail: grana@szfki.hu

Published online: 8 August 2004; doi:10.1038/nmat1190

Most research into microstructure formation during solidification has focused on single-crystal growth ranging from faceted crystals to symmetric dendrites. However, these growth forms can be perturbed by heterogeneities, yielding a rich variety of polycrystalline growth patterns. Phase-field simulations show that the presence of particulates (for example, dirt) or a small rotational–translational mobility ratio (characteristic of high supercooling) in crystallizing fluids give rise to similar growth patterns, implying a duality in the growth process in these structurally heterogeneous fluids. Similar crystallization patterns are also found in thin polymer films with particulate additives and pure films with high supercooling. This duality between the static and dynamic heterogeneity explains the ubiquity of polycrystalline growth patterns in polymeric and other complex fluids.

Many everyday materials, ranging from plastic grocery bags to airplane wings and cast-iron supporting beams for highway bridges, are fabricated by freezing liquids into polycrystalline solid structures. The properties and failure characteristics of these materials depend strongly on their microstructure, but the factors that determine this microstructure remain poorly understood[1].

As with other types of phase transitions, such as liquid–liquid phase separation[2], the geometrical forms of the ordering patterns can be remarkably insensitive to the molecular structure of the crystallizing species. Here, we thus adopt a coarse-grained order parameter (or 'phase field') description that can encompass this general phenomenon, while still retaining a thermodynamic and dynamical description of the ordering process in terms of measurable properties (diffusion coefficients of atomic species, surface energies, temperature, concentration, and so on). Our work extends previous treatments of crystallization by accounting for the freezing-in of local orientational fluctuations at the growth front that create new grains. We find that when this growth front nucleation (GFN) process is prevalent, single-crystal growth is transformed into polycrystalline growth.

Growth front nucleation (sometimes termed 'secondary nucleation') generates a spectrum of structures reflecting an interplay between the ordering effect of crystallization and the disordering effect of interfacial instabilities. In the absence of GFN, far from equilibrium, crystallization normally leads to symmetric dendrites similar to the structures of snowflakes (see refs 3 and 4 for a comparison of simulated and real dendrites). At the other end of the disorder spectrum, it is well known that intricately structured and locally disordered polycrystalline 'spherulite' patterns (see Fig. 1 in ref. 3) often form and these structures are ubiquitous in polymer materials in particular[3–5]. A wide range of patterns having intermediate complexity is found between these extreme morphologies and some representative ones are shown in Fig. 1. These examples encompass thin films of polymer blends[3,4], electrodeposited metal films[6] and single-component polymer films[7], so this type of pattern formation is clearly rather general. Our goal is to determine what role GFN plays in determining this type of morphological variation.

It has long been suggested that microscopic impurities might be responsible for the transition between single crystal and polycrystalline growth patterns[8]. Indeed, our previous work[9] has demonstrated that the presence of static heterogeneities (particles or 'dirt') can lead to

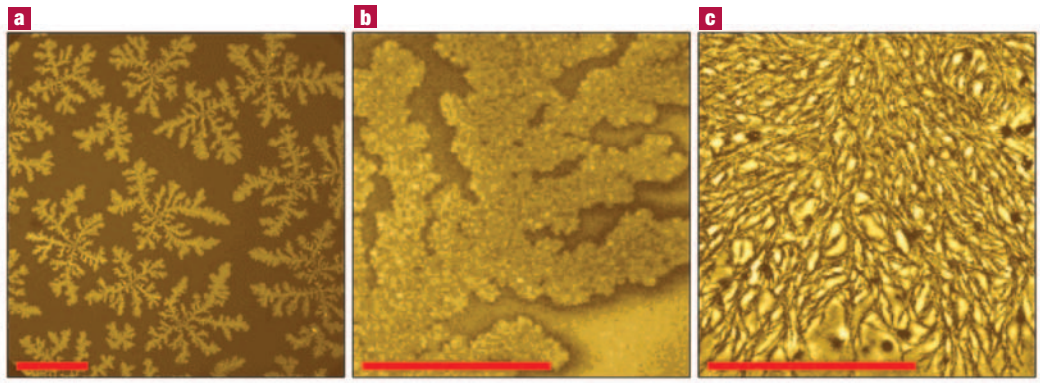

Figure 1 Thin-film polycrystalline growth morphologies. a, Disordered dendritic growth forms seen in polyethylene oxide (20 vol.%) and polymethyl methacrylate (80 vol.%) film of 90 nm thickness at 303 K (refs 3,4). **b**, Seaweed-like polycrystalline aggregate of electrodeposited Cu (image reprinted with permission from ref. 6). **c**, 'Fungus' morphology, as observed in the crystallization of thin (17 ± 2 nm) films of isotactic polystyrene at $T = 404$ K (ref. 7). The scale bars are **a**, 50 μm and **b**, **c**, 10 μm.

polycrystalline growth patterns through a sequential deflection of the tips of growing dendrites. However, this cannot be a general explanation of polycrystalline growth because spherulites have been observed to grow in liquids without particulates or detectable molecular impurities[10,11]. How can this be understood? A clue to this phenomenon can be found in the observations of Magill, who noted that spherulites only seem to appear in pure fluids when the viscosity is sufficiently large (~30–50 Pa s), typically corresponding to highly supercooled liquids[11]. What aspect of supercooled liquids could account for these observations?

Experimental studies of highly supercooled liquids have established that these fluids are spatially dynamically heterogeneous[12–18], that is, some molecules move orders of magnitude faster than those situated only nanometres away. Simulations of model glass-forming liquids in both two[19] and three[20] dimensions (as well as colloidal particle tracking measurements[16,17]) have given some insights into the geometrical form of these heterogeneous regions, but the phenomenon remains an active area of research.

This dynamic heterogeneity phenomenon has numerous consequences for the transport properties of these complex fluids. The most important transport properties of relevance to crystallization are the shear viscosity η and the molecular mobilities determined by the translational and rotational diffusion coefficients. These diffusion coefficients characterize the rate of molecular translation and rotation, directly controlling the manner by which molecules attach and align with the growing crystal[21–24]. It is a basic property of highly supercooled liquids that the ratio of the rotational and translational diffusion coefficients ($\chi = D_{rot}/D_{tr}$) decreases sharply (by orders of magnitude) from their nearly constant high-temperature values (χ_0)[14,15,21–24]. This 'decoupling' phenomenon means that molecules translate increasingly large distances before they rotationally decorrelate from their initial orientation[14,15,21–24].

Our previous study of polycrystalline growth in fluids having static heterogeneities (for example, clay particles) indicated that the essential mechanism of this type of growth was the stabilization of new crystal grains having the crystallographic orientation preferred by the particles rather than the parent crystal[9]. These symmetry-breaking events occur at the growth front, and only the local interactions between the particles and the crystallization front determine the nature of the grain-formation process. Analogously, we anticipate that the drop in χ, characteristic of highly supercooled liquids, can likewise enhance the growth of new grains, as misoriented crystal regions at the liquid–solid interface have difficulty aligning with the parent crystal. In other words, polycrystalline growth will arise if the reorientation of molecules is slow relative to the interface propagation. This argument implies that static heterogeneities and the mobility asymmetry ($\chi << \chi_0$) of supercooled liquids should give rise to a common tendency towards polycrystalline growth. In the present report, we investigate this hypothesis.

Field theoretical models have proved successful in describing phase separation and a wide range of pattern-formation processes involving critical dynamics[2]. Similar advances have been made extending this type of coarse-grained description to crystallization. Density functional[25] and phase-field theories[26,27] have been successfully developed to describe crystal nucleation[25,28–31] and morphological transitions[9,26,27]. Thus, the necessary theoretical and computational ingredients now exist for the formulation of non-equilibrium crystal growth with GFN naturally incorporated.

The phase-field model used here[28,29] builds on previous work for multigrain solidification[32,33], homogeneous (primary) crystal nucleation[28,29] and the modification of dendritic growth by particulate additives[9]. In this order-parameter description of crystallization, the material state is specified by the basic field variables ϕ and c describing the extent of local crystallization and composition at a given point in space $\mathbf{r}$, respectively. The shape of symmetric dendrites derives from an anisotropy introduced in either the liquid–solid surface energy or mobility. The energy cost of misorientation, which determines the grain-boundary energy, is necessarily associated with GFN, and requires the introduction of an additional local crystallographic orientation variable $\theta(\mathbf{r})$[28,32,33].

The free energy of the material is a functional of these 'minimal' field variables,

$$F = \int d\mathbf{r} \left\{ (\alpha^2/2)\, T \left| \nabla\phi \right|^2 + f(\phi, c) + f_{ori}(\phi, \nabla\theta) \right\}.$$

The magnitude of the square gradient term α characterizes the width of the diffuse crystal–liquid interface, a feature observed in experiment[34] and atomistic simulations[35]. Selection of a particular interface thickness sets the length scale of the simulations given below. The local free energy $f(\phi, c)$ has two minima (at $\phi = 0$, and $\phi = 1$), whose relative depth is the driving force for crystallization and is a function of both temperature, T, and concentration c. The orientational contribution to the free energy, $f_{ori} = HT\,[1 - p(\phi)]\,\left|\nabla\theta\right|$ quantifies the excess free energy due to inhomogeneities in crystal orientation in space, and, in particular, the grain-boundary misorientation[9,28]. The parameter H quantifies the energetic cost of misorientation[36], and $p(\phi)$, following the procedure

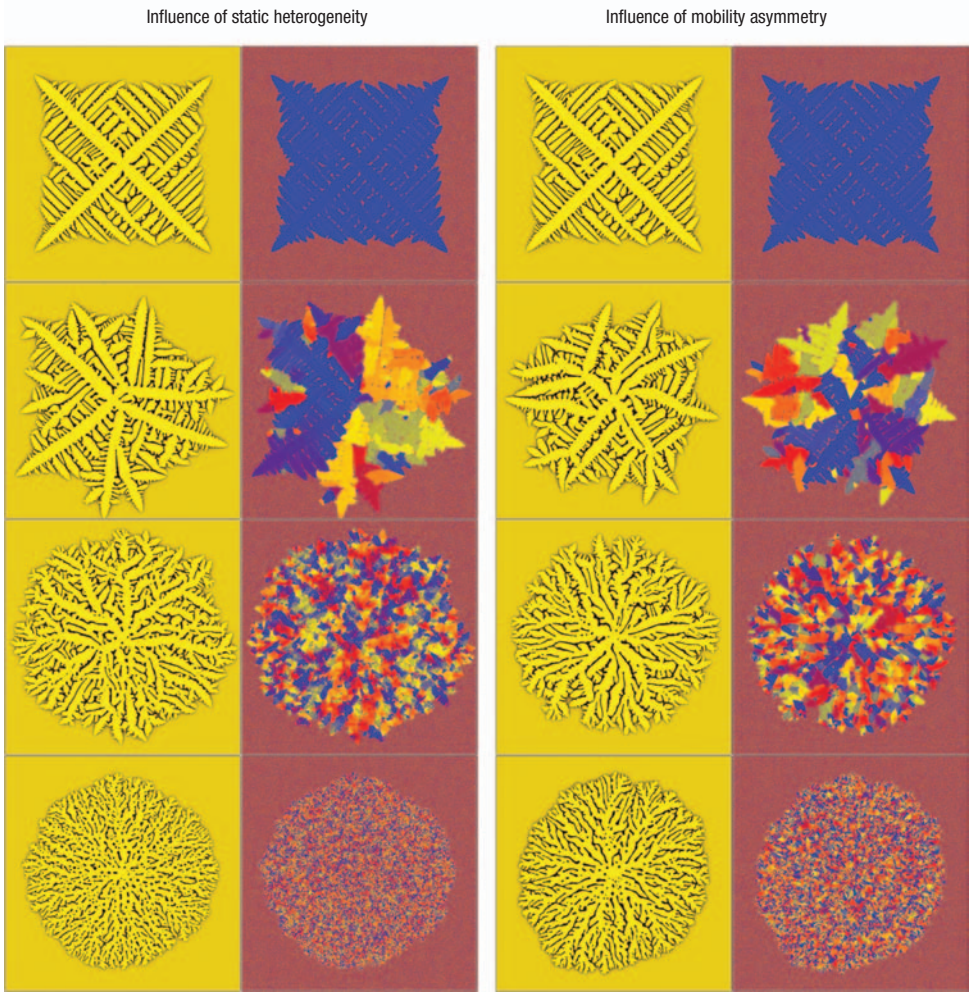

Figure 2 The effect of particulate additives (left two columns) and reducing the orientational-translational mobility ratio χ (right two columns) on the growth morphology. The 1st and 3rd columns are the chemical composition maps (solidus — yellow; liquidus — black). The 2nd and 4th columns are the orientation maps. (The colours denote crystallographic orientations: When the fast growth direction is diagonal, 30, or 60 degrees left, the grains are coloured blue, yellow, or red, respectively, and the intermediate angles are denoted by a continuous transition among these colours. Owing to the fourfold symmetry, orientations that differ by 90 degree multiples are equivalent.) In the left two columns, the number of single-pixel-sized orientation pinning centres varies from top to bottom as $N = 0$, 50,000, 200,000 and 800,000, respectively. In the right two columns, χ is multiplied by the factors 1, 0.4, 0.3 and 0.1, from top to bottom, respectively. The simulations have been performed with the physical properties of Ni–Cu at 1,574 K under a supersaturation of 0.8. Isotropic interfacial free energy, 50% anisotropy and a fourfold symmetry of the kinetic coefficient were assumed. The orientation-pinning centres have random position and orientation.

commonly used in phase-field theory[28,37], varies smoothly from 0 to 1 as ϕ changes from the solid to the liquid; $p(\phi) = \phi^3(10 - 15\phi + 6\phi^2)$. A similar approach has been used recently to investigate grain-boundary dynamics and multigrain growth[32,33,36]. This form of f_{ori} ensures that θ takes an essentially constant value (scaled between 0 and 1) in the solid, whereas in the liquid it fluctuates[28]. Notably, orientational ordering takes place at the diffuse interface simultaneously with the structural transition. This extension of the orientation field to the liquid accounts for the feature that the short-range order in the liquid and solid is usually similar, and can therefore be represented by a local value of θ (ref. 28). The time evolution is governed by relaxational dynamics and Langevin noise terms[28]. The timescales of the equations of motion are established by our choice of mobilities. Whereas the concentration mobility is directly related to the chemical diffusion coefficient, the phase-field mobility M_ϕ and orientational mobility M_θ must be chosen to capture properly the essential properties of a dynamically heterogeneous liquid.

The physical nature and origin of dynamic heterogeneity in supercooled liquids is an unsolved problem of condensed matter physics, and we seek to model the effect of this complex phenomenon based on minimal, plausible assumptions regarding our model parameters. Dynamic heterogeneities exist at the nanometre scale, but, as our model is coarse-grained, we do not model these fluctuations directly. Because χ/χ_0 is characteristically small in supercooled liquids, we postulate a corresponding reduction in the ratio of M_θ/M_ϕ to model the average effect of dynamic heterogeneity on global relaxation. This assumption is plausible because these coarse-grained mobilities are functions of their molecular counterparts. Moreover, recent experiment has shown that the rate of crystallization in highly supercooled liquids is proportional to D_{tr}, even under decoupling conditions[21,23,24]. In our model, the growth velocity scales linearly with M_ϕ, so consistency requires $M_\phi \propto D_{tr}$. Because we also expect that $M_\theta \propto D_{rot} \propto 1/\eta$, we arrive at $\chi \propto M_\theta/M_\phi$, as postulated above.

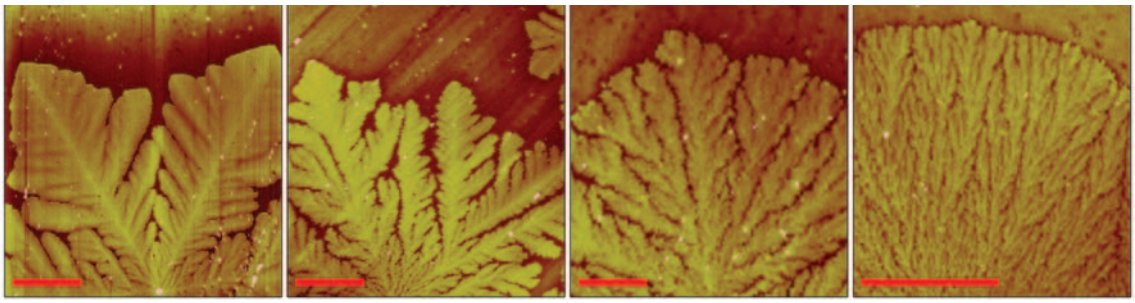

Figure 3 Growth morphologies observed during crystallization of pure isotactic polystyrene films (17 ± 2 nm thick) as a function of temperature[7]. Note the transition between the dendritic, disordered dendritic and seaweed morphologies with increasing undercooling. From left to right the temperature of crystallization is $T = 463$, 443, 433 and 423 K, respectively. The scale bars are 10 μm.

Our calculations were performed for the Ni–Cu system at 1,574 K. Previous work has established that the crystallization patterns that form in such miscible mixtures under conditions of high supersaturation and constant T are essentially equivalent to those formed in single-component fluids at high undercooling[37]. We choose the Ni–Cu system here because this is a classic case for which many of the model parameters are known. The orientation dependence of the molecular attachment kinetics is taken into account using an anisotropy function for the phase-field mobility, $M_\phi = M_{\phi,0}\{1 + \delta_0 \cos[m(\psi - \theta)]\}$, where δ_0 is a parameter characterizing the magnitude of the mobility anisotropy ($\delta_0 = 0$ for the isotropic case), and ψ is the inclination of the liquid–solid interface in the laboratory frame. Following our former comparisons between simulations and experiments on polymer films[9], we select a fourfold symmetry ($m = 4$), and unless stated otherwise, we use $\delta_0 = 0.5$, consistent in order of magnitude with molecular dynamics simulations for metals[38]. The filament-like crystallites forming in some polymeric matter, however, imply rather a twofold symmetry and a large kinetic anisotropy, which will also be explored. The calculations were performed at a rather high supersaturation, $S = (c_L - c)/(c_L - c_S) = 0.8$, where c_L, c_S and c are the concentrations at the liquidus, solidus and the initial homogeneous liquid mixture, respectively. Following our previous work[9], we adopt a simple model of the particulates ('dirt'). They are represented here by orientational pinning centres (small areas of random, but fixed, orientation). This picture economically describes morphological changes deriving from particle–dendrite interactions[9]. The calculations were performed on a 2,000 × 2,000 rectangular grid (26.4 μm × 26.4 μm for the parameters chosen above), on a cluster of commodity personal computers consisting of 75 nodes and a server machine.

The effect of particulate additives on dendritic morphology is shown in Fig. 2. As the number of the particles increases, the single-crystal dendrite transforms through secondary grain formation at the growth front into an increasingly polycrystalline object with a 'random' internal structure. First, the symmetric dendrite gives way to dizzy dendrites forming by sequential tip deflection[9]. This morphology is followed by seaweed growth at higher particle densities due to the randomization of the orientation caused by the small crystallites. Similar changes can be seen in the orientation map and morphology when χ is reduced (Fig. 2). The reference value of χ was selected to be large enough to ensure single-crystal growth. When χ is sufficiently small, the system can no longer establish the same orientation along the perimeter of the growing crystal, as suggested by our initial hypothesis. Thus, GFN gives rise to a transition to polycrystalline growth.

Experiments with sufficient resolution to probe the local orientation of the disordered crystallization structures shown in Figs 1 and 3 are apparently not currently available. However, we note that a dendrite to polycrystalline seaweed transition has been observed in Zn electrodeposition pattern formation[39], where the patterns are similar to Fig. 1b. Moreover, it is well known that this type of morphological transition can occur in the absence of GFN by simply reducing the anisotropy of the interfacial free energy (see Fig. 3) so that the tip of the crystal tends to split during growth[40–45]. Thus, the seaweed morphology forms both as a single crystal[40–45] and polycrystalline aggregate[6,39,46,47], implying that one cannot distinguish crystalline from polycrystalline seaweed structures by morphology alone (see Fig. 4). Quenching of orientational defects into the crystal offers an attractive explanation for the polycrystalline seaweed morphology that probably describes many cases in practice, although further measurements are required to assess the generality of this mechanism of disordered growth.

A final, dramatic example of the analogous roles played by static heterogeneities and low-χ/χ_0 supercooled liquids (foreign particles and frozen orientational defects) is displayed in Fig. 5. This figure shows the conversion of a needle-shaped single crystal to a polycrystalline morphology that we have termed 'fungus'. The needle crystal forms in our simulation because of a high kinetic anisotropy ($\delta_0 = 0.995$), but this symmetric, single-crystal structure becomes randomized through branching caused either by foreign particles or by frozen-in orientational defects. This branching restores structural isotropy at large scales, while retaining intricate crystal structure at relatively fine scales. The spontaneous formation of this type of morphology in pure isotactic polystyrene thin films under high undercooling is shown in Fig. 1c (ref. 7).

The duality between the effects of dynamic heterogeneities as they influence χ versus static heterogeneities provides a fundamental insight into the prevalence of polycrystalline growth in polymeric materials, and the similarity of these growth patterns to those of small-molecule liquids containing 'dirt'. In each of these heterogeneous fluids, new grains are nucleated at the growth front yielding a polycrystalline growth form. New grains can be initiated either by incorporation of particles with a particular orientation preference or by the quenching-in of orientational defects near the liquid–solid interface.

We also note that dynamic clustering is not restricted to glass-forming materials, but is characteristic of colloidal[16], dipolar, ionic and other associating fluids[48,49]. These systems should likewise exhibit mobility asymmetry[50] (low-χ/χ_0), and thus a tendency towards polycrystalline growth should occur as a general phenomenon in complex fluids. Finally, our simulations imply that nucleating agents introduced to control the size and distribution of crystallites may very well yield a variety of unanticipated polycrystalline growth morphologies. These structural changes have implications for the

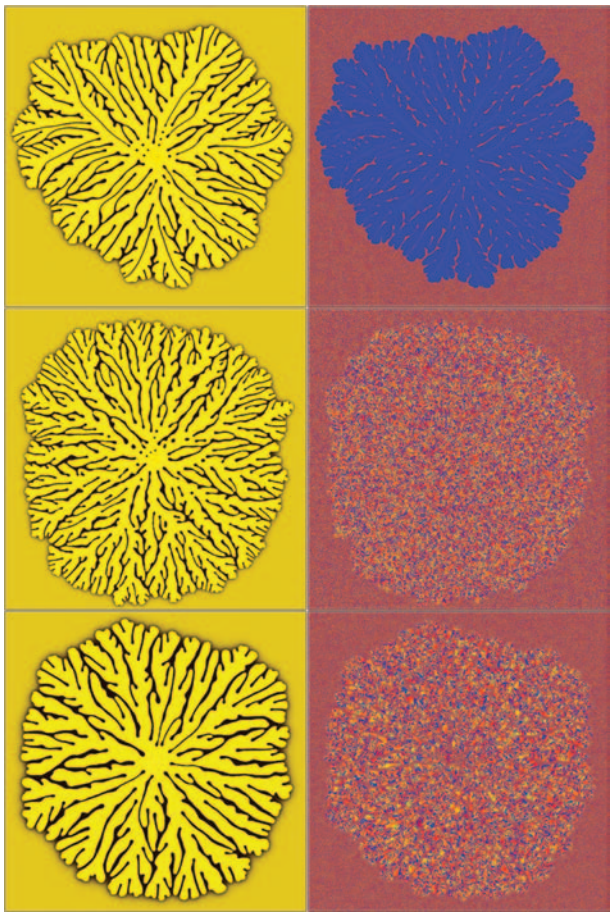

Figure 4 The seaweed morphology may develop either as a single crystal[40–45] or as a polycrystalline object[6,39,46,47], as recovered by our phase-field simulations. Single-crystal seaweed (top) forms when both the interface free energy and kinetic coefficient are isotropic or close to isotropic. Polycrystalline seaweed can be obtained by either introducing foreign particles (400,000 single-pixel-sized orientation pinning centres; centre row) or by reducing the orientational mobility (by a factor of 50; bottom). The calculations were performed with isotropic interface free-energy and kinetic coefficient with a supersaturation, $S = 0.78$. The colouring is the same as for Fig. 2. Note that similar morphologies occur in the anisotropic case, if the growth form consists of a large number of fine grains (see Fig. 2).

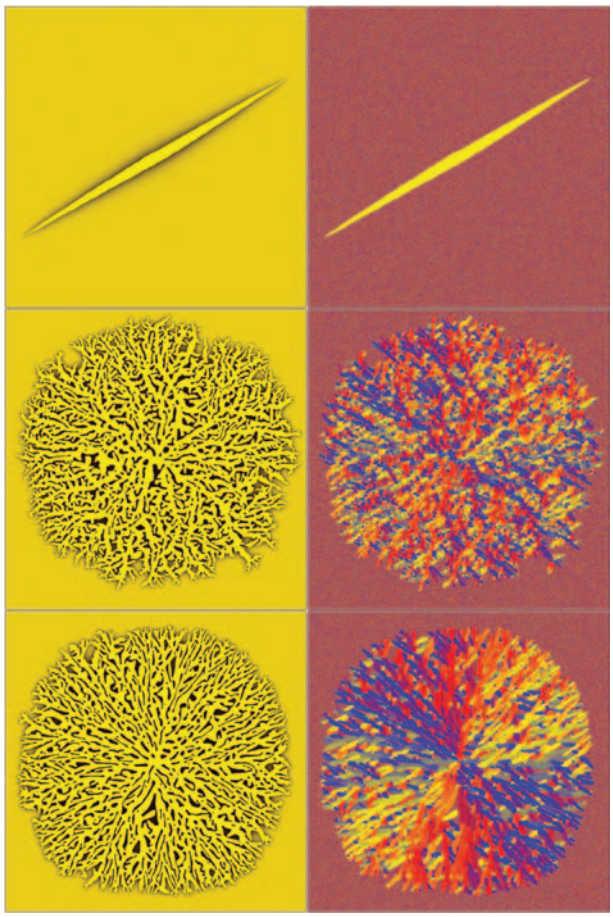

Figure 5 Single-crystal needle (top) and polycrystalline 'fungi' produced by introducing foreign particles (centre) or by reducing χ (bottom) as predicted by the phase-field theory. In the bottom row, χ has been reduced by a factor of 5 to mimic the effect of high supercooling. $N = 250{,}000$ single-pixel-sized orientation pinning centres have been introduced into the simulation shown in the centre row. The interfacial free-energy is isotropic whereas the anisotropy of the phase-field mobility is 99.5%, and has a twofold symmetry ($m = 2$). The colouring of the orientation map is an adaptation of the scheme shown in Fig. 2 for twofold symmetry: When the fast growth direction is upwards, 60, or 120 degrees left, the grains are coloured red, blue or yellow, respectively, and the intermediate angles are denoted by a continuous transition among these colours. Owing to twofold symmetry, orientations that differ by 180-degree multiples are equivalent.

properties and structural stability of these and similar imperfectly ordered structural materials encountered in nature and manufacturing.

Received 16 February 2004; accepted 29 June 2004; published 8 August 2004.

References

1. Cahn, R. W. *The Coming of Materials Science* (Pergamon, Oxford, 2001).
2. Gunton, J. D., San Miguel, M. & Sahni, P. in *Phase Transitions and Critical Phenomena* Vol. 8 (eds Domb, C. and Lebowitz, J. L.) 267–466 (Academic, London, 1983).
3. Ferreiro, V., Douglas, J. F., Warren, J. A. & Karim, A. Nonequilibrium pattern formation in the crystallization of polymer blend films. *Phys. Rev. E* **65,** 042802 (2002).
4. Ferreiro, V., Douglas, J. F., Warren, J. A. & Karim, A. Growth pulsations in symmetric dendritic crystallization in polymer blend films. *Phys. Rev. E* **65,** 051606 (2002).
5. Woodward, A. E. *Atlas of Polymer Morphology* (Hanser, New York, 1988).
6. Fleury, V. Branched fractal patterns in non-equilibrium electrochemical deposition from oscillatory nucleation and growth. *Nature* **390,** 145–148 (1997).
7. Beers, K. L., Douglas, J. F., Amis, E. J. & Karim, A. Combinatorial measurement of crystallization growth rate and morphology in thin films of isotactic polystyrene. *Langmuir* **19,** 3935–3940 (2003).
8. Keith, H. D. & Padden, F. J. Crystallization of polymers from the melt and the structure of bulk semicrystalline polymers. *J. Appl. Phys.* **34,** 2409–2421 (1963).
9. Gránásy, L. *et al.* Growth of 'dizzy dendrites' in a random field of foreign particles. *Nature Mater.* **2,** 92–96 (2003).
10. Ryshchenkow, G. & Faivre, G. Bulk crystallization of liquid selenium. *J. Non-Cryst. Solids* **87,** 221–235 (1988).
11. Magill, J. H. Spherulites: A personal perspective. *J. Mater. Sci.* **36,** 3143–3164 (2001).
12. Tracht, L. *et al.* Length scale of dynamic heterogeneities at the glass transition by multidimensional nuclear magnetic resonance *Phys. Rev. Lett.* **81,** 2727–2730 (1998).
13. Russell, E. V. & Israeloff, N. E. Direct observation of molecular cooperativity near the glass transition. *Nature* **408,** 695–68 (2000).
14. Ediger, M. D. Spatially heterogeneous dynamics in supercooled liquids. *Ann. Rev. Phys. Chem.* **51,** 99–128 (2000).
15. Chang, I. & Sillescu, H. Heterogeneity at the glass transition: Translational and rotational self-diffusion. *J. Phys. Chem. B* **101,** 8794–8801 (1997).
16. Weeks, E. R., Crocker, J. C., Levitt, A. C., Schofield, A. & Weitz, D. A. Three dimensional imaging of structural relaxation near the colloidal glass transition. *Science* **287,** 627–631 (2000).
17. Kegel, W. K. & van Blaaderen, A. Direct observation of dynamical heterogeneities in colloidal hard-sphere suspensions. *Science* **287,** 290–293 (2000).
18. Bennemann, C., Donati, C., Baschnagel, J. & Glotzer, S. C. Growing range of correlated motion in a polymer melt on cooling towards the glass transition. *Nature* **399,** 246–249 (1999).
19. Mel'cuk, A. I., Ramos, R. A., Gould, H. Klein, W. & Mountain, R. D. Long-lived structures in fragile glass-forming liquids. *Phys. Rev. Lett.* **75,** 2522–2525 (1995).

20. Donati, C. *et al.* Stringlike cooperative motion in a supercooled liquid. *Phys. Rev. Lett.* **80,** 2338–2341 (1998).
21. Ngai, K. L., Magill, J. H. & Plazek, D. J. Flow, diffusion and crystallization of supercooled liquids: Revisited. *J. Chem. Phys.* **112,** 1887–1892 (2000).
22. Rössler, E. Indication for a change in diffusion mechanism in supercooled liquids. *Phys. Rev. Lett.* **65,** 1595–1598 (1990).
23. Masuhr, A., Waniuk, T. A., Busch, R. & Johnson, W. L. Time scales for viscous flow, atomic transport, and crystallization in the liquid and supercooled liquid states of $Zr_{41.2}Ti_{13.8}Cu_{12.5}Ni_{10.0}Be_{22.5}$. *Phys. Rev. Lett.* **82,** 2290–2293 (1999).
24. Swallen, S. F., Bonvallet, P. A., McMahon, R. J. & Ediger, M. D. Self-diffusion of *tris*-naphthylbenzene near the glass transition temperature. *Phys. Rev. Lett.* **90,** 015901 (2003).
25. Oxtoby, D. W. Density functional methods in the statistical mechanics of materials. *Annu. Rev. Mater. Res.* **32,** 39–52 (2002).
26. Boettinger, W. J., Warren, J. A., Beckermann, C. & Karma, A. Phase-field simulation of solidification. *Annu. Rev. Mater. Res.* **32,** 163–194 (2003).
27. Hoyt, J. J., Asta, M. & Karma, A. Atomistic and continuum modeling of dendritic solidification. *Mater. Sci. Eng. Rep. R* **41,** 121–163 (2003).
28. Gránásy, L., Börzsönyi, T. & Pusztai, T. Nucleation and bulk crystallization in binary phase field theory. *Phys. Rev. Lett.* **88,** 206105 (2002).
29. Gránásy, L., Börzsönyi, T. & Pusztai, T. Crystal nucleation and growth in binary phase field theory. *J. Cryst. Growth* **237–239,** 1813–1817 (2002).
30. Gránásy, L. & Pusztai, T. Diffuse interface analysis of crystal nucleation in hard-sphere liquid. *J. Chem. Phys.* **117,** 10121–10124 (2002).
31. Gránásy, L. *et al.* Phase field theory of crystal nucleation in hard sphere liquid. *J. Chem. Phys.* **119,** 10376–10382 (2003).
32. Kobayashi, R., Warren, J. A. & Carter, W. C. Vector-valued phase field model for crystallization and grain boundary formation. *Physica D* **119,** 415–423 (1998).
33. Kobayashi, R., Warren, J. A. & Carter, W. C. Modeling grain boundaries using a phase-field technique. *Physica D* **140,** 141–150 (2000).
34. Huisman, W. J. *et al.* Layering of a liquid metal in contact with a hard wall. *Nature* **390,** 379–381 (1997).
35. Davidchack, R. L. & Laird, B. B. Simulation of the hard-sphere crystal-melt interface. *J. Chem. Phys.* **108,** 9452–9462 (1998).
36. Warren, J. A., Kobayashi, R., Lobkovsky,, A. E. & Carter, W. C. Extending phase field models of solidification to polycrystalline materials. *Acta Mater.* **51,** 6035–6058 (2003).
37. Warren, J. A. & Boettinger, W. J. Prediction of dendritic growth and microsegregation patterns in a binary alloy using the phase-field method. *Acta Met. Mater.* **43,** 689–703 (1995).
38. Hoyt, J. J. & Asta, M. Atomistic computation of liquid diffusivity, solid-liquid interfacial free energy, and kinetic coefficient in Au and Ag. *Phys. Rev. B* **65,** 214106 (2002).
39. Grier, D., Ben-Jacob, E., Clarke, R. & Sander, L. M. Morphology and microstructure in electrochemical deposition of zinc. *Phys. Rev. Lett.* **56,** 1264–1267 (1986).
40. Kobayashi, R. Modeling and numerical simulation of dendritic growth. *Physica D* **63,** 410–423 (1993).
41. Ihle, T. & Müller-Krumbhaar, H. Fractal and compact growth morphologies in phase transitions with diffusion. *Phys. Rev. E* **49,** 2972–2991 (1994).
42. Taguchi, K. *et al.* Growth shape of isotactic polystyrene crystals in thin films. *Polymer* **42,** 7443–7447 (2001).
43. Utter, B. & Bodenschatz, E. Dynamics of low anisotropy morphologies in directional solidification. *Phys. Rev. E* **66,** 051604 (2002).
44. Akamatsu, S., Faivre, G. & Ihle, T. Symmetry-broken double fingers and seaweed patterns in thin-film directional solidification of a nonfaceted cubic crystal. *Phys. Rev. E* **51,** 4751–4773 (1995).
45. Lovinger, A. J. & Cais, R. E. Structure and morphology of poly(trifluoro-ethylene). *Macromolecules* **17,** 1939–1945 (1984).
46. Ben-Jacob, E., Deutscher, G., Garik, P., Goldenfeld, N. D. & Lareah, Y. Formation of dense branching morphology in interfacial growth. *Phys. Rev. Lett.* **57,** 1903–1906 (1986).
47. Lereah, Y. *et al.* Morphology of Ge:Al thin films: Experiments and model. *Phys. Rev. E* **49,** 649–656 (1994).
48. Dudowicz, J., Freed, K. F. & Douglas, J. F. Flory-Huggins model of equilibrium polymerisation and phase separation in the Stockmayer fluid. *Phys. Rev. Lett.* **92,** 045502 (2003).
49. Kumar, S. K. & Douglas, J. F. Gelation in physically associating polymer solutions. *Phys. Rev. Lett.* **87,** 188301 (2001).
50. Bedrov, D., Smith, G. D. & Douglas, J. F. Influence of self-assembly on dynamical viscoelastic properties of telechelic polymer solutions. *Europhys. Lett.* **59,** 384–390 (2002).

Acknowledgements

We thank Vincent Ferreiro (CNRS), Kathryn Beers (NIST) and Vincent Fleury (CNRS) for providing the images shown in Figs 1 and 4. This work has been supported by contracts OTKA-T-037323, ESA PECS No. 98005, and by the EU Integrated Project IMPRESS. T.P. acknowledges support by the Bolyai János Scholarship.
Correspondence and requests for materials should be addressed to L.G.

Competing financial interest

The authors declare that they have no competing financial interests.